Data-Driven Health Management of Electrical Vehicle Battery Systems

**Final Report
August 2018**

MIDWEST
TRANSPORTATION
CENTER **MTC**

IOWA STATE UNIVERSITY
Institute for Transportation

Technical Report Documentation Page

1. Report No.	2. Government Accession No.	3. Recipient's Catalog No.
4. Title and Subtitle Data-Driven Health Management of Electrical Vehicle Battery Systems		**5. Report Date** August 2018
		6. Performing Organization Code
7. Author(s) Guangxing Bai, Pingfeng Wang, Krishna Krishnan, and Janet Twomey		**8. Performing Organization Report No.**
9. Performing Organization Name and Address Wichita State University Department of Industrial and Manufacturing Engineering 1845 Fairmount Street Box 35 Wichita, KS 67260		**10. Work Unit No. (TRAIS)**
		11. Contract or Grant No. Part of DTRT13-G-UTC37
12. Sponsoring Organization Name and Address Midwest Transportation Center 2711 S. Loop Drive, Suite 4700 Ames, IA 50010-8664 Wichita State University 1845 Fairmount Street Wichita, KS 67260	U.S. Department of Transportation Office of the Assistant Secretary for Research and Technology 1200 New Jersey Avenue, SE Washington, DC 20590	**13. Type of Report and Period Covered** Final Report
		14. Sponsoring Agency Code
15. Supplementary Notes Visit www.intrans.iastate.edu for color pdfs of this and other research reports.		

16. Abstract

The objectives of this research were to conduct theoretical and experimental investigations to develop a new battery health management paradigm based on a novel, self-cognizant dynamic system (SCDS) approach to predict and prevent failures of safety-critical battery systems (e.g., lithium plating and thermal runaway) for electric vehicles (EVs) and hybrid electric vehicles (HEVs) and develop an onboard diagnostics tool and alarm system for early awareness of these potential impending failures.

This research developed a technique that can adaptively recognize the dynamic characteristics of an operating battery system over time without relying on expensive, time-consuming battery tests for the prediction and prevention of safety-critical battery system failures. Battery failure prognostics employing the proposed SCDS-based health management paradigm can not only account for normal battery capacity fading over time but also identify abnormal safety-critical failures that usually happen in a relatively shorter time period.

17. Key Words battery—dynamic systems—electric vehicle—health management—safety		**18. Distribution Statement** No restrictions.	
19. Security Classification (of this report) Unclassified.	**20. Security Classification (of this page)** Unclassified.	**21. No. of Pages** 37	**22. Price** NA
Form DOT F 1700.7 (8-72)		**Reproduction of completed page authorized**	

DATA-DRIVEN HEALTH MANAGEMENT OF ELECTRICAL VEHICLE BATTERY SYSTEMS

Final Report
August 2018

Principal Investigator
Pingfeng Wang, Associate Professor
Industrial and Manufacturing Engineering, Wichita State University

Co-Principal Investigators
Krishna Krishnan, Professor and Chair
Janet Twomey, Professor and Associate Dean
Industrial and Manufacturing Engineering, Wichita State University

Research Assistant
Guangxing Bai

Authors
Guangxing Bai, Pingfeng Wang, Krishna Krishnan, and Janet Twomey

TABLE OF CONTENTS

LIST OF FIGURES

LIST OF TABLES

ACKNOWLEDGMENTS

A previous version of this report was published as a journal article:

Bai, G. and P. Wang. 2016. An Internal State Variable Mapping Approach for Li-Plating Diagnosis. *Journal of Power Sources*, Vol. 323, pp. 115–124. https://www.sciencedirect.com/science/article/pii/S0378775316305766.

EXECUTIVE SUMMARY

The objectives of this research were to conduct theoretical and experimental investigations to develop a new battery health management paradigm based on a novel, self-cognizant dynamic system (SCDS) approach to predict and prevent failures of safety-critical battery systems (e.g., lithium plating and thermal runaway) for electric vehicles (EVs) and hybrid electric vehicles (HEVs) and develop an onboard diagnostics tool and alarm system for early awareness of these potential impending failures.

This research developed a technique that can adaptively recognize the dynamic characteristics of an operating battery system over time without relying on expensive, time-consuming battery tests for the prediction and prevention of safety-critical battery system failures. Battery failure prognostics employing the proposed SCDS-based health management paradigm can not only account for normal battery capacity fading over time but also identify abnormal safety-critical failures that usually happen in a relatively shorter time period.

A systematic, multiphysics simulation platform was developed for safety-critical battery failures. Based on battery electrochemical kinetics, a battery model was developed to describe internal variables such as electrolyte concentration or electrical potential in both solid and solution phases during electrochemical reactions.

INTRODUCTION

With the prevalence of portable electronics and hybrid electric vehicles (HEVs), lithium-ion (Li-ion) batteries have drawn significant attention due to their notable advantages over other types of batteries: high energy density, slow self-discharging rate, and no memory effect. Meanwhile, the risk of various safety-critical battery failures has become an important issue to be addressed for battery applications. Development of an advanced battery management system (BMS) could significantly mitigate the risk of potential battery failures. An advanced BMS is designed to acquire electrical data, control the operational environment, monitor internal states, predict future degradation, and protect batteries from unexpected failures (Plett 2004). For a BMS, the state-of-charge (SoC) and state-of-health (SoH) are two important parameters indicative of battery health condition; therefore, accurately estimating them becomes a paramount task in BMS development (Zhang and Lee 2011).

A tremendous amount of work has been done to improve performance of the BMS technique (Hu et al. 2011, Miranda and Hong 2013, Zheng et al. 2013, Santhanagopalan et al. 2006, Charkhgard and Farrokhi 2010, Bai et al. 2014, Bai et al. 2015, Sun et al. 2010). Hu et al. (2011) developed a multiscale framework with an extended Kalman filter for SoC and SoH estimation. Miranda and Hong (2013) developed an integrated model for high-power cylindrical batteries to improve the SoC accuracy under extended operating conditions. Zheng et al. (2013) developed a mean-plus-difference model to estimate SoC. Santhanagopalan et al. (2006) estimated the SoC for a Li-ion cell using an online approach. Charkhgard and Farrokhi (2010) proposed a data-driven method to estimate a cell's SoC. Bai et al. (2014, 2015) developed a self-cognizant dynamic system approach for prognostics and health management of Li-ion batteries. And Sun et al. (2010) developed a health diagnosis method based on approximate entropy.

Since most battery failure modes involve very complicated internal electrochemical reactions, accurate modeling and analysis of a specific battery failure mode is extremely challenging. Therefore, detecting and diagnosing those failure modes have become a very important research task for broad battery applications, because enabling remedial strategies and implementing protections accordingly can avoid battery failures and even prevent hazardous system damages due to these failures. One of many failure modes for Li-ion batteries, lithium (Li) plating is a safety-critical failure mode that happens at the negative electrode in the charging process (Doughty and Roth 2012). Once Li plating happens, several irreversible side reactions occur inside the battery where numerous active Li-ions lose their activity, which could significantly reduce the capacity of the cells, thus leading to sudden battery capacity loss. Meanwhile, the plated lithium metal around the negative electrode could form a dendritic structure that could cause physical damage to the separator and electrodes, leading to short circuits or other related critical battery failures.

Since Fuller and Doyle established the electrochemical battery model using porous electrode and concentration solution theories (Fuller et al. 1994), several models have been further developed to investigate the internal dynamics of Li-ion batteries. Due to the complexity and inefficiency of the electrochemical model, a single-particle model has been developed to improve computational efficiency without significantly compromising accuracy (Ning and Popov 2004,

Santhanagopalan et al. 2006). Employing these electrochemical simulation models, capacity fade has been investigated as the most important battery degradation performance mode (Ramadass et al. 2004, Ning et al. 2006). In addition, thermal models have also been proposed along with the developed electrochemical model by Cai and White (2010) and Guo et al. (2011). Recently, researchers have begun investigating battery failure modes using the electrochemical model. Perkins et al. (2012) developed a control-oriented, reduced-order model to determine Li plating by estimating several important battery parameters through simulations. Legrand et al. (2014) presented a new method to access the charging process of a Li-ion battery by characterizing the Li plating effect. However, the existing work has failed to consider the impact of changes to a battery's internal state due to aging over time. Since most related work has been built upon the foundation of the battery electrochemical model, or Doyle-Fuller-Newman (DFN) model (Chaturvedi et al. 2010), which employs a system of partial differential equations (PDEs) to describe electrochemical principles in Li-ion batteries, coefficients in these PDEs are essential to estimate correct values under various battery operating conditions. As a battery system experiences a wide variety of external circumstances in service, several physical and chemical coefficients in the PDEs could vary in a large enough range to change the system's behavior. In this case, employing fixed coefficients to analyze battery system behavior is inappropriate. The related time-varying coefficients in a Li-ion battery system, denoted as internal state variables (ISVs), include diffusion coefficients, reaction rate, conductivity, and so on. With regard to a specific failure mode, a certain set of coefficients could be influenced to induce or mitigate the occurrence of battery failures. By identifying failure-related coefficients over time, such as those key factors that activate the Li plating failure mechanism, battery system behavior could be better understood.

A few studies reported in the literature have focused on battery parameter identification by applying different approaches to given battery models. Santhanagopalan et al. (2007) developed an approach that employs Levenberg-Marquardt optimization and the Markov chain Monte Carlo (MCMC) method to estimate parameters in the DFN model. Speltino et al. (2009) used a two-step approach to identify battery parameters, in which the cathode equilibrium potential function is first approximated from observations of open circuit voltage (OCV), and battery tests are performed to identify battery parameters of interest. Forman et al. (2012) employed a generic algorithm (GA) to identify battery parameters with the DFN model and used the fisher information criterion to perform an identifiability analysis. In existing studies, a full DFN model has been generally used for parameter identification and has been combined with other simulation or heuristic algorithms such as MCMC and GA. The computational burden for parameter identification is usually very high based on the complexity of numerical calculation of PDEs in the DFN model, and meanwhile, the implementation of MCMC or GA also adds a large amount of computational work, which together prevents these approaches from being used in practical applications.

To address these challenges, this research presents a new ISV mapping approach to identify battery parameters and capture battery system failures due to Li plating. In the developed ISV mapping approach, an artificial neural network (ANN) model is first constructed to model battery system response with respect to different designed battery parameters. With the developed ANN model, weights can be used to enhance correlation with battery parameters in the original DFN model. A Kriging-based surrogate model can then be built to map the neural

network (NN) weights to the battery's ISVs. The constructed Kriging model can be further used to identify battery parameters in real-time using online measurement data during the battery service process.

After identifying battery ISVs, a new criterion to detect the occurrence of Li plating was proposed. To demonstrate the developed ISV mapping approach for Li plating diagnosis, the experiment used COMSOL Multiphysics software to simulate Li plating and then information about the concentration of electrodes to analyze local effects and the onset timing.

This report is organized as follows:

- Chapter 2 introduces work related to the Li-ion battery electrochemical model and the ANN and Kriging models used for the development of the ISV mapping approach.
- Chapter 3 details the developed ISV mapping approach.
- Chapter 4 presents the mechanisms of Li plating and the new approach for its detection.
- Chapter 5 shows the experiments implemented using COMSOL Multiphysics software and the subsequent results that illustrate Li plating diagnosis using the developed approach.
- Chapter 6 covers the results and accomplishments of this project.
- Appendix A provides the details of the DFN or pseudo two-dimensional (P2D) model equations.

RELATED WORK

The Doyle-Fuller-Newman Model

The DFN model, or pseudo two-dimensional (P2D) model, was developed from the battery electrochemical model using the ohmic porous electrode theory and Bulter-Volmer kinetics by Fuller et al. (1994). Based on the battery electrochemical kinetics, the P2D model can describe internal variables such as concentration or potential in both the solid phase and solution phase. The P2D model consists of three regions: negative electrode, separator, and positive electrode. In each electrode, there are two phases: the solid phase (consisting of porous electrode particles) and the solution phase (being full of electrolyte). During regularly charging/discharging processes, the current will force the Li-ions to extract from particles of one electrode, move through the electrolyte, and intercalate into particles of the other electrode. The P2D model describes this behavior of Li-ions, which follows diffusion kinetics (Chaturvedi et al. 2010).

As shown in Figure 1, a generic P2D model structure is used to study the battery's internal states.
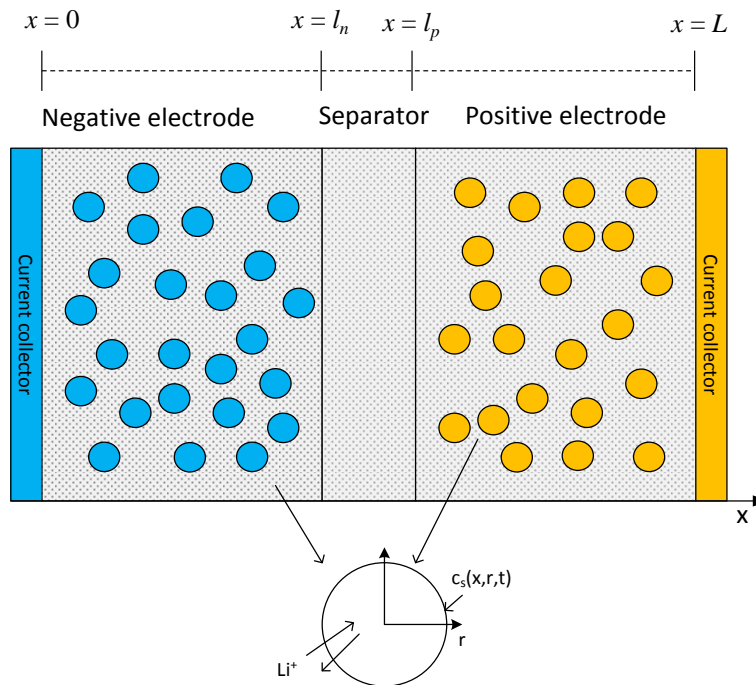
Bai and Wang 2014b, Copyright © 2014, IEEE, Reprinted with permission.

Figure 1. Two-dimensional structure of a Li-ion battery

This model only considers Li^+ diffusion dynamics in the electrolyte along the horizontal x-axis and Li^+ exaction/intercalation behaviors in spherical particles along the radius r-axis. PDEs are employed to solve for the electrolyte concentration, electrolyte potential, solid phase concentration, and solid phase potential along different locations on the x-axis and r-axis. Detailed equations of the P2D model are presented in Appendix A.

Artificial Neural Network Model

Artificial neural networks have been designed for various applications, such as pattern recognition, prediction, optimization, function approximation, and control. A typical ANN is constructed with artificial neurons that consist of nodes and weighted links between neuron inputs and outputs. Based on different network architectures, ANN can be classified into two categories: feed-forward networks and recurrent networks.

In this research, one of the most commonly used feed-forward networks, namely a multilayer perceptron (MLP), was employed to approximate the system response for a dynamic battery system. In an MLP, several neuron nodes are used to compose three types of network layers, with generally one input layer, one or multiple hidden layers, and one output layer. The information is propagated directly from the input layer through hidden layers to the output layer. The information propagation process is realized by using the activation function, which transforms the activation level of a neuron into an output signal. There are a number of common activation functions in use with an ANN, of which the sigmoid function is most widely used. A general ANN model is showed in Figure 2.
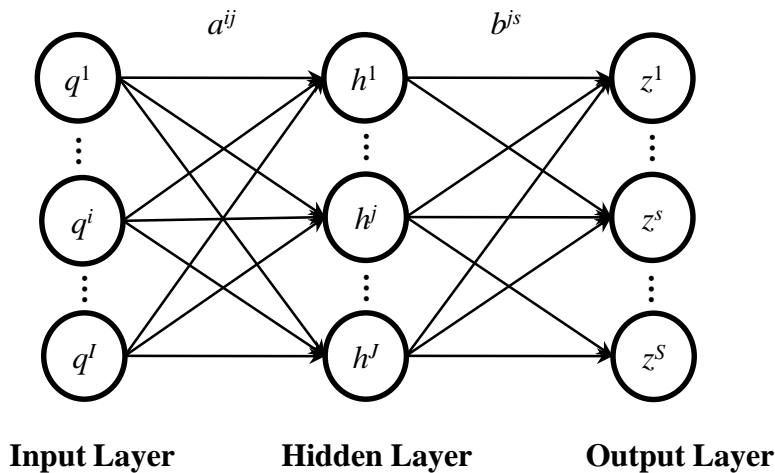
Figure 2. General neural network model

Figure 2 shows the structure of the developed MLP, where q is the NN input with node index 1 to I, h is the NN hidden nodes with node index 1 to J, z is the NN output with index 1 to s, a^{ij} is the weight connecting input node i to hidden node j, and b^{js} is the weight connecting hidden node j and output node s.

In this research, an ANN is constructed to intelligently learn the response of the P2D model with multiple coefficients, then a Kriging model is used to find the relationship between ANN weights and P2D model coefficients.

Kriging-Based Surrogate Model

This subsection introduces the Kriging technique. Kriging, also called Gaussian process regression, was originally developed as a fundamental geostatistical method and has been used for several decades. It is a probabilistic method for interpolating values modeled by a Gaussian process based on observed measurements.

Based on various stationary properties of global means in the Kriging model, different methods have been developed to apply to practical situations with varying degrees of assumed stationarity. The classical methods include simple Kriging for a known constant mean, ordinary Kriging for an unknown constant mean, and universal Kriging for a general polynomial mean function. In this research, ordinary Kriging was employed to address the special ISV mapping problem.

The Kriging model is usually presented as follows:

$$y(\mathbf{x}) = f(\mathbf{x}) + S(\mathbf{x}) \tag{1}$$

where $\mathbf{x}$ is an n-dimensional vector for n design variables, $y(\mathbf{x})$ is an unknown function that the Kriging model tends to express, $f(\mathbf{x})$ is a global mean function that can provide several options such as a constant term or a polynomial function, and $S(\mathbf{x})$ is the realization of a stochastic process with zero mean and variance σ^2, which represents a local deviation from the global mean. In this research, a constant μ is used for the global mean function $f(\mathbf{x})$.

The correlation between $S(\mathbf{x}_i)$ and $S(\mathbf{x}_j)$ is related to the distance between samples $\mathbf{x}_i$ and $\mathbf{x}_j$. It is represented as follows:

$$Corr(S(\mathbf{x}_i), S(\mathbf{x}_j)) = \sigma^2 R(\mathbf{x}_i, \mathbf{x}_j) \tag{2}$$

where $R(\mathbf{x}_i, \mathbf{x}_j)$ is an $n \times n$ correlation matrix, and the distance between $\mathbf{x}_i$ and $\mathbf{x}_j$ is not the Euclidean distance that has the same weights for all design variables. The distance, with additional weighted values, can be expressed as follows:

$$d(\mathbf{x}_i, \mathbf{x}_j) = \sum_{k=1}^{n} \alpha_k \left| \mathbf{x}_i^k - \mathbf{x}_j^k \right|^2 \tag{3}$$

where α_k are the undetermined weights used to match the model, and $\mathbf{x}_i^k$ and $\mathbf{x}_j^k$ are the kth design variables. Given the distance of two samples, the (i, j) entry of correlation matrix R can be written as follows:

$$R(\mathbf{x}_i, \mathbf{x}_j) = \exp(-d(\mathbf{x}_i, \mathbf{x}_j)) \tag{4}$$

For a new interpolated sample of x_{new}, the prediction of the Kriging model is given as follows:

$$y(\mathbf{x}_{new}) = \mu' + \mathbf{r}^{\mathbf{T}}(\mathbf{x}_{new}) \mathbf{R}^{-1}(\mathbf{y} - \mathbf{1}\mu')$$

(5)

where $\mathbf{r}(x_{new})$ is a correlation vector where the ith element is as follows:

$$r_i(\mathbf{x}_{new}) = Corr(S(\mathbf{x}_{new}), S(\mathbf{x}_i))$$

(6)

and the mean estimate μ' is as follows:

$$\mu' = (\mathbf{1}^{\mathbf{T}}\mathbf{R}^{-1}\mathbf{1})^{-1}\mathbf{1}^{\mathbf{T}}\mathbf{R}^{-1}\mathbf{y}$$

(7)

Also, the estimate of the variance, σ' is defined by the following:

$$\sigma' = \frac{\left(\mathbf{y\text{-}1}\mu'\right)^{\mathbf{T}} \mathbf{R}^{-1}(\mathbf{y\text{-}1}\mu')}{n}$$

(8)

Among all equations, the undetermined parameter in the Kriging model is $\boldsymbol{\alpha}$ in Equation (3). In order to estimate this parameter, the maximum likelihood estimation (MLE) method is employed to address this problem. The likelihood function is expressed as follows:

$$Likelihood(\mu', \sigma', \boldsymbol{\alpha}) = -\frac{n}{2}\ln(2\pi) - \frac{n}{2}\ln(\sigma'^2) - \frac{1}{2}\ln(|\mathbf{R}|) - \frac{1}{2\sigma'^2}(\mathbf{y} - \mathbf{1}\mu')^{\mathbf{T}}\mathbf{R}^{-1}(\mathbf{y\text{-}1}\mu')$$

(9)

In order to maximize Equation (9), several numerical methods (such as the Newton-Gauss method) are selected to approximate model parameter $\boldsymbol{\alpha}$. For a given value of $\boldsymbol{\alpha}$, μ' and σ' are able to be updated accordingly. The calculation routine then repeats, calculating these three coefficients until the likelihood function converges to a stable maximum value.

THE DEVELOPED ISV MAPPING APPROACH

Identification of Battery Model Parameters

As previously mentioned, inherent system parameters must be identified and confirmed so that internal system states can be estimated during battery system dynamical processes. However, determining the coefficients in PDEs is a very challenging problem, especially in a complex PDE form or system of PDEs (Santhanagopalan et al. 2007, Speltino et al. 2009, Schmidt et al. 2010). Meanwhile, existing studies generally employ the full or reduced-order P2D models and rely on numerical techniques to iteratively estimate required parameter values. To apply existing methods for the estimation of PDE coefficients, computational burden is generally extremely high for even a single battery parameter. Mathematically, the presented problem for a PDE can be expressed as follows:

$$F(\mathbf{x}, t, u, \frac{\partial u}{\partial x_1}, ..., \frac{\partial u}{\partial t}; \boldsymbol{\theta}) = 0 \tag{10}$$

where F is a linear function of u and its derivatives, $\mathbf{x} = (x_1, ... x_p)^T$ is a p-dimensional argument, and $\boldsymbol{\theta}$ is the parameter vector that relates to primary interest of this research.

The present problem of the Li-ion battery electrochemical model is more complex than Equation (10). First, the P2D model includes several PDEs from Equation (A.1) to (A.16), as shown in Appendix A, to construct a system of PDEs in order to describe the entire Li-ion battery system. Second, the variable $\mathbf{u}$ in Equation (10) is unobservable in the system of PDEs for the Li-ion battery, which increases the difficulty in using observations to estimate PDE parameters. For the sake of addressing these challenges, an ISV mapping approach was proposed. In this new approach, a reduced-order model was developed for the P2D model to reveal dependencies between observed voltage and variables in the battery model, and a surrogate model was applied to reduce the computational complexity of the system of PDEs.

Reduced-Order Model for the Li-ion Battery

This subsection presents the reduced-order model for the Li-ion battery P2D model. Equation (A.3) in Appendix A shows that output voltage is equal to the difference between potentials at two boundaries, $x = 0$ and $x = L$. Since the x variables don't need to be considered when calculating output voltage, the existing PDE can be reduced to an ordinary differential equation (ODE) for electrode potential:

$$\mathrm{L}\Phi(x, t) = f(x, t, I(t), \boldsymbol{\theta}) \rightarrow \frac{\mathrm{d}\Phi_{x=0, L}(t)}{\mathrm{d}t} = f(t, I(t), \boldsymbol{\theta}) \tag{11}$$

Thus, Equation (11) simplifies the variable Φ to be a variable only related to time. By discretizing this equation, the following can be obtained:

$$\Phi_{x=L,k} - \Phi_{x=L,k-1} = \Delta t \times f(I_k, \boldsymbol{\theta}) \tag{12}$$

Finally, the voltage at time index k can be summarized as follows:

$$V_k = G(I_k, V_{k-1}, \boldsymbol{\theta}) \tag{13}$$

Equation (13) implies that the output voltage at time point k only depends on the input current at time k, the voltage at previous time point k-1, and the related coefficients in the PDEs. Equation (13) can significantly reduce the complexity of the original system of PDEs and easily generalize the relationship between system input and output. Using Equation (13), it would be easy to employ a surrogate model to replace the reduced model and estimate system response with required accuracy.

Battery ISV Mapping

This subsection presents the proposed methodology of the developed approach. To realize the time-varying parameters and diffusion coefficients in the governing PDEs, a two-stage method was designed to solve this problem.

In the first stage, a surrogate model was constructed to approximate PDE system response. A surrogate model has two advantages compared to the original, full PDE model. First, under an accepted accuracy level, a surrogate model could largely reduce computational complexity. Second, a surrogate model provides explicit weights in model equations, which could be utilized to map time-varying coefficients in the PDE model.

In the developed approach, an NN model was selected from surrogate models. The NN model can be written as follows:

$$y(x) = \sum_{i=1}^{I} a_i \varphi \left(\sum_{j=1}^{J} w_{ij} x_j + b_j \right), \ and \ \mathbf{W} = [a_i, w_{ij}, b_j]^{\mathbf{T}} \tag{14}$$

where a, w, and b are all weights inside the NN model, x is the input of the NN model, and i and j represent the number of hidden nodes and input nodes, respectively. And φ as the sigmoid function can be expressed as follows:

$$\varphi(\xi) = \frac{1}{1 + e^{-\xi}} \tag{15}$$

In order to surrogate the reduced battery model, the input of the NN model is assigned to be I_k and V_{k-1}; the output of the NN model is V_k.

To fit the battery model, the Levenberg-Marquardt algorithm is used to optimize the NN weights to ensure the validation of the NN model. The optimization is expressed as follows:

$$\underset{\mathbf{W}_{cycle}}{\textbf{Minimize}}:\sum_{k}(V_{k,cycle}-y(\mathbf{W}_{cycle}))^2 \tag{16}$$

where *cycle* represents the cycle index, k is the time index in a specific cycle, y represents the estimates of the NN model, and V is the true system output.

Apparently, the trained weights $\mathbf{W}$ in the NN model have a strong correlation with coefficient $\boldsymbol{\theta}$, since both of them are the only parameters in their respective models. Therefore, building an accurate mapping from $\mathbf{W}$ to $\boldsymbol{\theta}$ would assist in determining the values of the PDE coefficients. The mapping can be written as follows:

$$g:\mathbf{W}\rightarrow\boldsymbol{\theta} \tag{17}$$

In this mapping, the dimension of input is regulated by the number of hidden nodes in the predefined NN model, and the dimension of output is determined by the number of coefficients in the PDEs. The mapping solution in this research is based on the assumption that the Kriging model has powerful estimation skills when tackling interpolation problems.

Flowchart of the ISV Mapping Approach

The procedure of the developed approach is illustrated in Figure 3.
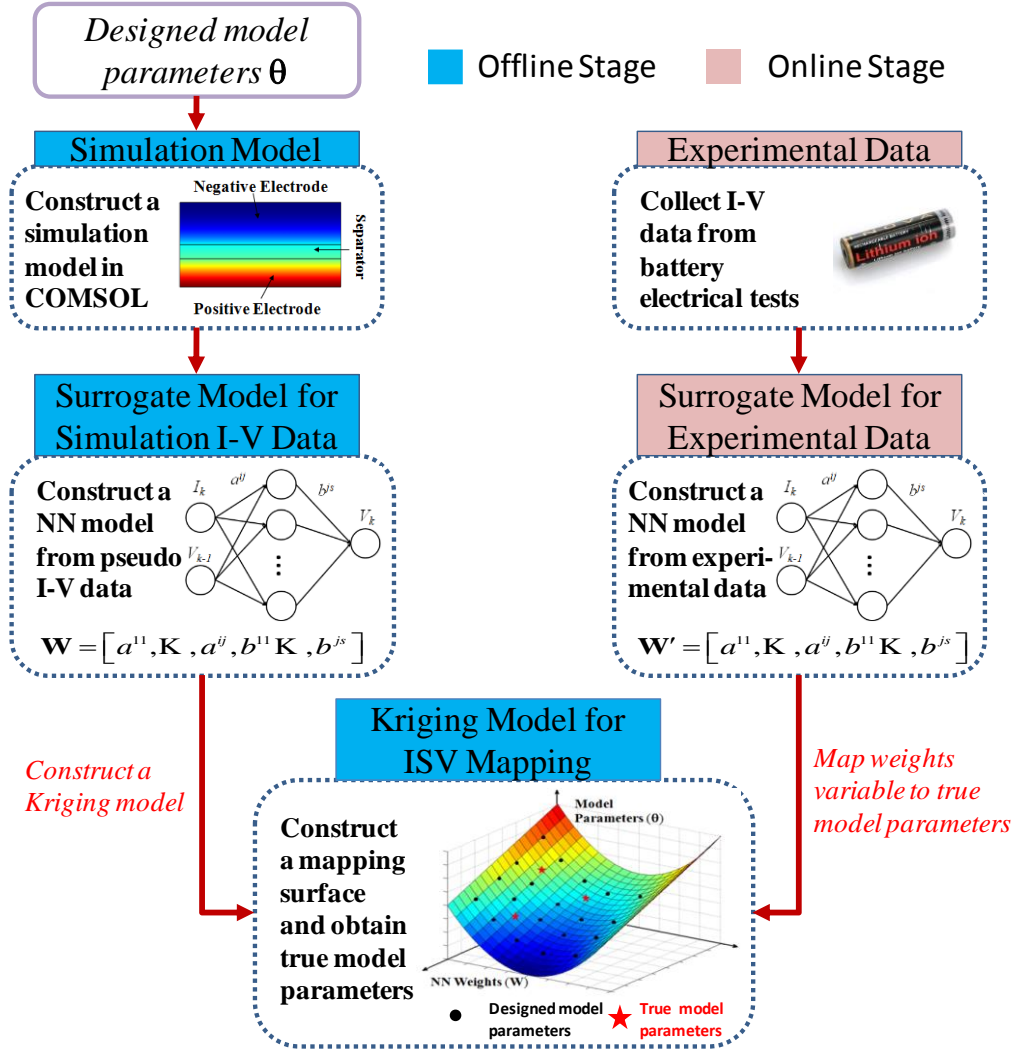
Figure 3. Procedure of the developed ISV mapping approach

As the figure shows, the whole approach was divided into offline and online stages. The basic idea was to utilize the mapping relationships between the NN weights and diffusion coefficients revealed by the Kriging model to estimate current diffusion coefficients in the test battery using experimental data.

In the offline stage, the test battery characteristics, such as materials in the electrodes and electrolyte, geometry of the battery structure, and several other fixed parameters, were designed in a COMSOL Multiphysics model; this model was then able to execute the simulated battery cycling experiments, which could easily provide system responses under different, designed current and diffusion coefficients. After obtaining system behavior with several I-V curves, an NN model instead of a full PDE model was employed to approximate the I-V relationships. As mentioned previously, a Levenberg Marquardt algorithm was used to optimize the NN model until the required accuracy level was reached. Due to the direct relationship between the weights

11

from the NN model and the diffusion coefficients from the aimed PDE model, a Kriging model was employed to approximate the mapping relationship between weight $\mathbf{W}$ and coefficient $\boldsymbol{\theta}$.

In the online stage, the test battery had to be set up to go through a charging and discharging experiment to obtain the real experimental data. The battery experiment first performed a discharging profile until the voltage dropped under 3.2 V, which is the stop voltage for discharge. The battery could be considered deeply discharged in this case. Then a constant charging current was applied to the discharged battery, and at the same time the battery tester recorded the measurement signals (i.e., current and voltage). In the same procedure, the measured I-V curve was also plugged into the NN model to get trained until the error level was met. Obtaining the weights $\mathbf{W'}$ from the newly trained NN, the variable $\mathbf{W'}$ was plugged into the designed Kriging model to get the prediction of diffusion coefficient $\boldsymbol{\theta'}$. Since the diffusion coefficient $\boldsymbol{\theta'}$ represents the battery's current state, which could affect Li plating occurrence, the Li plating could be predicted according to the given diffusion coefficients.

LI PLATING MECHANISM

Electrochemical Explanations for the Li Plating Mechanism

During extreme operating conditions when charging, Li-ion batteries could experience an aging phenomenon due to Li plating. Under these conditions, which make reduction reactions occur more easily, metallic lithium could be deposited on the surface of the negative electrode instead of intercalating into it. The Li plating phenomenon generally occurs during the charging process under two specific conditions: charging at a high current or low temperature.

When Li-ion batteries are charging at a high current, the active Li-ion will extract from the positive electrode, move across the separator, and intercalate into the negative electrode. However, the high current makes the extraction rate larger than the intercalation rate, causing side reactions to occur that turn Li-ions to metallic lithium on the surface of the negative electrode particles. Similarly, a low temperature will slow down the intercalation rate on the surface of the negative electrode and result in Li plating on the negative electrode. These side reactions when Li plating occurs are concluded as follows:

$$xLi^+ + Li_\delta C_6 + xe^- \rightarrow Li_{\delta+x} C_6 \tag{18}$$

$$(1-x)Li^+ + (1-x)e^- \rightarrow (1-x)Li \downarrow \tag{19}$$

Reaction (18) is the regular insertion reaction in which xLi^+ (x represents the fraction of charge carriers) is inserted into the graphite structure formed by six carbon atoms C_6. Reaction (19) is the Li plating side reaction that causes $(1-x)Li^+$ to form metal lithium and be plated on the surface of the negative electrodes.

Since the metallic lithium has very active properties, it will continue having other side reactions with substances in the electrolyte, which are shown as follows:

$$R + Li \downarrow \rightarrow Li - R \tag{20}$$

where R represents the carbonate solvent electrolyte. This side reaction indicates that metallic lithium could be rapidly oxidized by the substances of the electrolyte and form an additional solid electrolyte interface (SEI). The new SEI layer could stop the further side reactions between the plated lithium metal and other oxidizers. As a consequence, the newly formed plated lithium metal will be protected gradually and take a dendritic form that would cause more hazardous damages.

Li Plating Occurrence Model for Diagnosis

As described previously, Li plating occurs when the extraction rate of Li^+ from positive electrodes exceeds the intercalation rate of Li^+ into negative electrodes. To create the Li plating model, several additional assumptions should be made: (1) Equation (20) is the only side reaction occurring in the charging process (the other side reactions are ignored) and (2) the Li^+ concentration gradient on the surface of the electrodes approximates to the extraction or intercalation rate, because the Li plating only relates to the variation of Li^+ concentration on the surface of the electrode particles. Besides, in order to compare two rates in local areas, the average concentration gradient must be computed in a specific area. Based on this fact, the researchers defined the two equations to demonstrate the extraction/intercalation rate as follows:

$$R_{ex} = \frac{\partial \overline{c}_{s,surf,p}}{\partial t}$$

(21)

$$R_{in} = \frac{\partial \overline{c}_{s,surf,n}}{\partial t}$$

(22)

where R_{ex} and R_{in} represent the extraction rate and intercalation rate, respectively, as $c_{s,surf,p}$ and $c_{s,surf,n}$ represent the solid phase concentration on the surface of different electrode particles, which can be obtained by $c_{s,surf} = c_s|_{r=Rp}$ for both electrodes according to Equation (A.10) in Appendix A. After calculating Equations (21) and (22) at different locations and time points, the extraction and intercalation rates can be obtained. According to the mechanism of Li plating, Li plating occurs only when the following is satisfied:

$$|R_{ex}| > |R_{in}|$$

(23)

When Equation (23) is satisfied at a specific location or time point, the Li plating could be considered to happen.

LI PLATING DIAGNOSIS EMPLOYING THE ISV MAPPING APPROACH

2D Battery Model Case

In this subsection, the weights-mapping approach was implemented for the case of a 2D Li-ion battery. The results show that the local effects of Li plating are due to the impact of the battery's geometry.

The 2D battery model implemented using COMSOL Multiphysics V4.4 was based on the electrochemical principles of a Li-ion battery. With the same materials, this model was built in three regions: the positive electrode (pink area), the negative electrode (grey area), and the separator (green area). Two current collectors cover the two electrodes. For experimental purposes, the current collector of the positive electrode was cut over half the areas to enhance the Li plating effects on those local areas. Thus, the battery model was divided into two parts according to the partially covered current collector. This unbalanced design of the current collectors was intended to enlarge the difference between the extraction and intercalation rates in the local test area. Consequently, a large of amount of computational effort was saved in this study because the Li plating phenomenon was easily generated. The geometry of the 2D Li-ion battery model is shown in Figure 4.
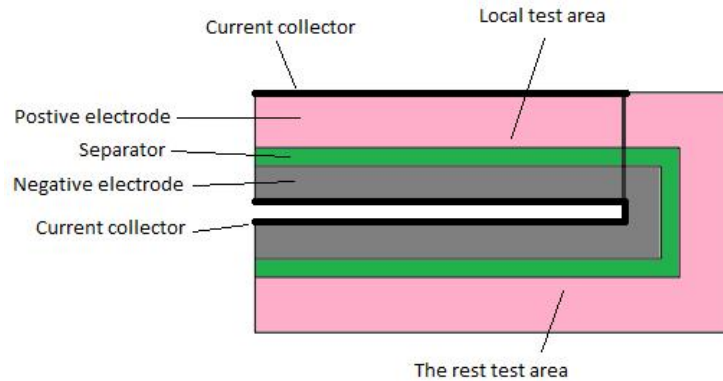
Bai and Wang 2014b, Copyright © 2014, IEEE, Reprinted with permission.

Figure 4. 2D Li-ion battery geometry in COMSOL Multiphysics V4.4

In this study, the designed diffusion coefficients in different electrodes vary from 1e-12 to 1e-15 m2/s according to surveys with different measurement techniques in the current literature (Ramadesigan et al. 2009). For each diffusion coefficient, the PDE solver was designed to uniformly sweep the coefficient range at 20 steps, which implies that the total number of parameter combinations was 20×20 = 400 groups. Using all parameter combinations, 400 charging cycles were able to be generated to implement the developed approach. By applying the weights-mapping approach, an NN model was used to surrogate the designed battery model, and 400 weights vectors were trained corresponding to the related parameter combinations. Then, 50 groups of parameter combinations were randomly chosen to validate the developed approach.

Li Plating Diagnosis Using ISV Mapping

By applying 50 groups of testing parameter combinations, the developed approach was implemented to approximate the true PDE parameters. Figure 5 shows the estimations of the diffusion coefficients at two electrodes in the 2D Li-ion battery model.
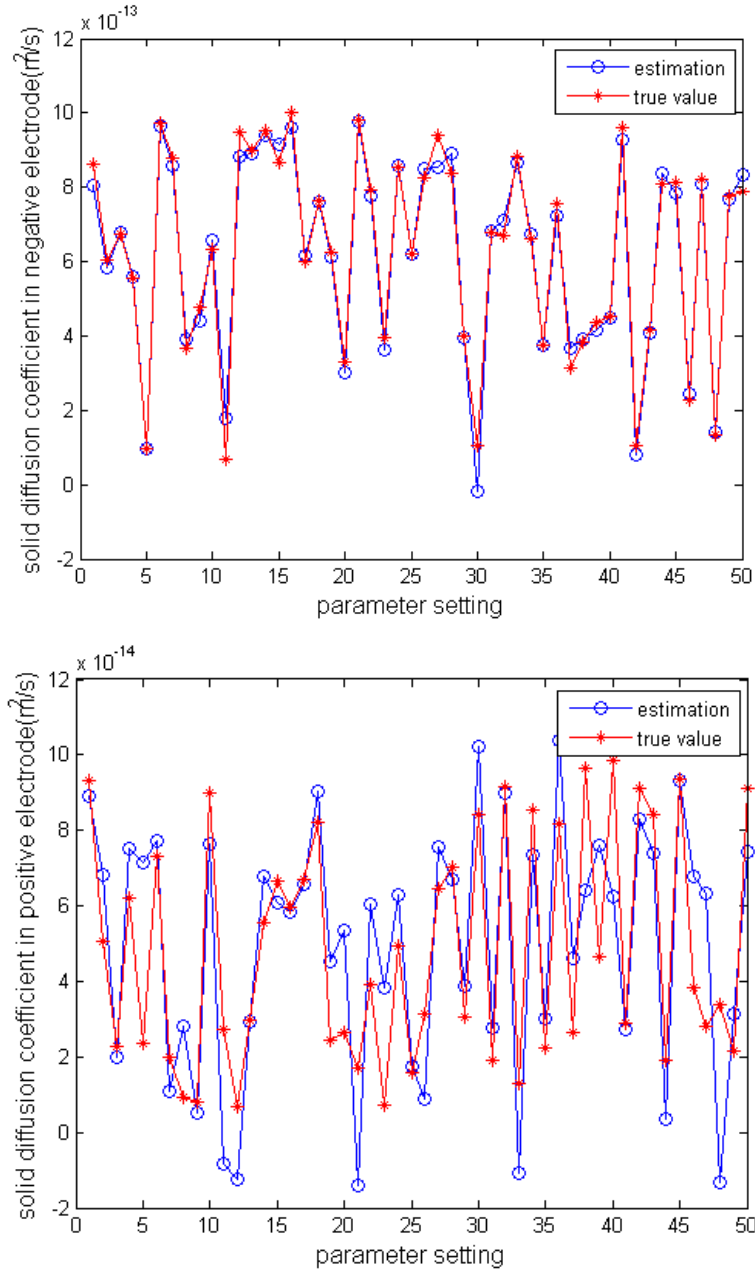
Figure 5. Estimation of diffusion coefficient in negative electrode (top) and estimation of diffusion coefficient in positive electrode (bottom)

The results shown in Figure 5 and Table 1 indicate that the developed approach was able to achieve a high accuracy of approximation.

Table 1. Accuracy of the ISV mapping approach

Diffusion Coefficient Estimation	Mean Square Error	Relative Error
At negative electrode	1.3471e-27	1.6414 %
At positive electrode	4.0126e-28	4.2338 %

It is observed that the mean square error (MSE) or relative error (RE) of the diffusion coefficient at the positive electrode is larger than the one at the negative electrode. This fact is attributed to the ANN model output, namely the voltage, which has less sensitivity to the diffusion coefficient at the positive electrode. Thus, the weights of the ANN model have a weaker link to the diffusion coefficient at the positive electrode compared to the one at the negative electrode. The equations for MSE and RE are expressed as follows:

$$MSE = \frac{1}{N}\sum_{i=1}^{N}\left(Y_i^{approx} - Y_i^{ob}\right)^2 \tag{24}$$

$$RE = 100\% \times \frac{1}{N}\sum_{i=1}^{N}\left|1 - \frac{Y_i^{approx}}{Y_i^{ob}}\right| \tag{25}$$

where N is the total number of approximations and Y_i^{approx} and Y_i^{ob} are the approximation and true value, respectively.

After obtaining the approximations of the diffusion coefficients, the PDE solver was able to obtain the concentration information in different electrodes. For easy occurrence of the Li plating, the related parameters were adjusted to proper values. The initial SoC was set to 90%, which means that the battery was close to fully charged. Then, the battery charging simulation underwent different diffusion coefficient combinations. Since the diffusion coefficients could significantly impact the Li-ion concentration performance in different electrodes, randomly coupled coefficients were selected to indicate the Li plating occurrence under various conditions. Figure 6 shows the concentration gradient performance with different combinations of parameters.
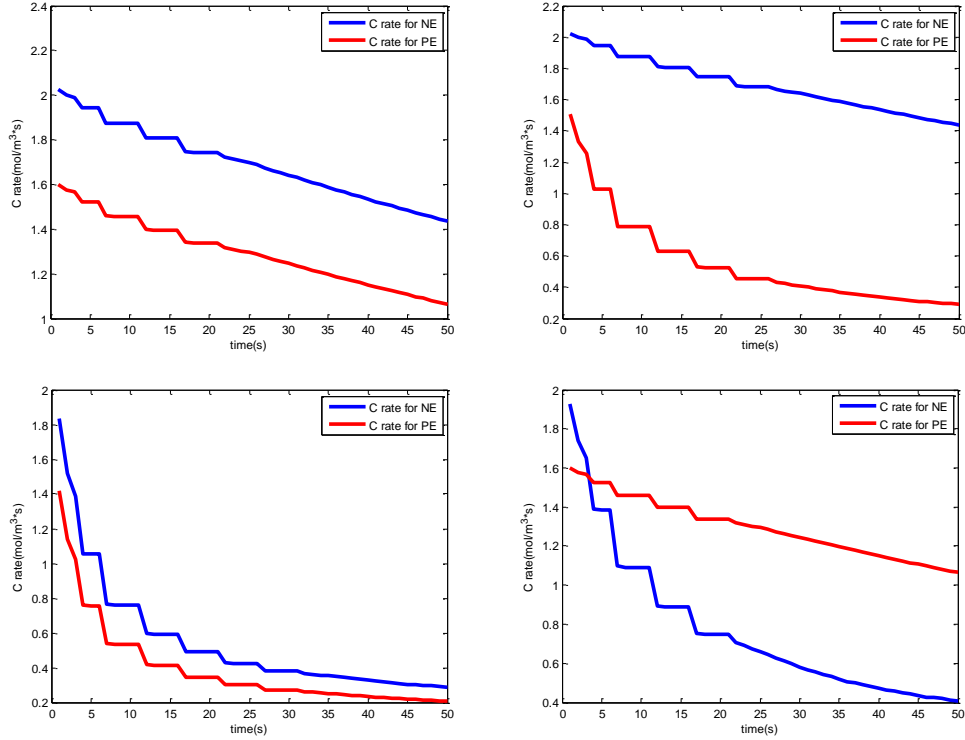
Figure 6. Concentration gradient with different combinations of parameters: Concentation gradient D_n=2.013e-13 and D_p=1.121e-13 (top left), concentration gradient with D_n=2.021e-13 and D_p=5.012e-14 (top right), concentration gradient with D_n=1.211e-14 and D_p=4.986e-15 (bottom left), and concentration gradient with D_n =1.122e-14 and D_p=5.124e-14 (bottom right)

In each chart, the blue curve and red curve represent the Li-ion concentration gradient for the negative and positive electrodes, respectively. In the top left graph in Figure 6, the specific diffusion coefficients make the concentration gradients of both electrodes parallel to each other, and the value of the positive electrode is much smaller than that of the negative electrode. In this case, Li plating would not happen during the entire time scale. Meanwhile, the top right graph in Figure 6 shows that the concentration gradient of the positive electrode diverges from that of the other electrode, which indicates that Li plating is unlikely to occur in the future. In the bottom left graph in Figure 6, the concentration gradients of both electrodes are shown to be close to each other and converging, which indicates that Li plating could happen in the future at the point when one curve intersects the other. But in the circumstance shown in the bottom right graph in Figure 6, the blue curve intersects the red curve at time t = 4s, indicating that the concentration gradient of the positive electrode has exceeded that of the negative electrode. In the case of coupled coefficients, Li plating would occur after the intersection and be diagnosed by the proposed approach.

18

PROJECT RESULTS AND ACCOMPLISHMENTS

Objective and Results

Accurate estimation of the SoC and SoH for an operating battery for electric vehicles, as a critical task for battery health management, greatly depends on the validity of battery models. Due to the variability and uncertainties involved in battery design, manufacturing, and operation, developing a generally applicable battery physical model is a big challenge. To eliminate the dependency of SoC and SoH estimation on battery physical models, a generic data-driven technique was investigated for battery health management.

The proposed technique tries to integrate an ANN with a dual-extended Kalman filter (DEKF) algorithm to capture the time-variant dynamics of an operating battery system for health management. The ANN is trained offline to model the battery terminal voltages to be used by the DEKF. With the trained ANN, the DEKF algorithm can then be employed online for SoC and SoH estimation, where voltage outputs from the trained ANN can be used in DEKF state-space equations to replace the battery physical model.

Battery failures, such as sudden capacity loss, could cause catastrophic damage. Li plating, which causes short circuiting and capacity loss, was one of critical failure modes addressed in this research. Based on the mechanisms of Li plating, this research developed a new approach to detect the occurrence of Li plating for an operating battery system. Experiments were conducted to validate and demonstrate the effectiveness of the proposed model-free technique for battery health management. The simulation of Li plating was conducted using the COMSOL Multiphysics software simulation tool. A new Li plating occurrence model was then developed and implemented under different conditions.

The researchers developed a general, model-free technique and a related practical application tool set for electric vehicle battery health management. Also, the researchers conducted this study to validate and demonstrate their new Li plating occurrence model. Experimental results indicated that the local effects and onset timing of Li plating could be potentially identified through the developed model. Moreover, the researchers developed a self-cognizant, dynamic system approach for the health management of Li-ion batteries. The researchers employed a multiphysics simulation-based approach for the Li plating failure mechanism investigation and developed a diagnostics framework for Li plating associated failure identification and forecasting.

The researchers have generalized the self-cognizant, dynamic system concept to form a general prognostics and health management (PHM) framework that is more suitable for processing time series sensory signals and conducting remaining useful life predictions. The researchers have also continued investigation of the safety-critical battery failure mode and successfully developed a diagnosis approach based on the ISV of the battery systems, such as the diffusion coefficient for Li plating failure identification. With this breakthrough, addressing the most safety-critical failure modes of lithium-ion batteries for electric vehicle (EV) and HEV applications becomes possible.

19

Meanwhile, the researchers have also been working on the experimental demonstration of the developed methodology on a laboratory scale, and the experimental facilities have been gradually developed in place at the research team's laboratory at Wichita State University.

The researchers have scaled up the investigation of the safety-critical battery failure mode from the battery cell level to battery pack/system level and have studied battery life models as well as battery cost models in relation to battery operating conditions. The researchers have developed an empirical battery life model based on the four critical battery operational parameters: temperature, depth of discharge, charging rate, and cycling frequency. This developed battery life model will enable the researchers to investigate further how a battery energy storage system (BESS) should be operated so that it can preserve a longer life.

Opportunities for Training and Development

The researchers have been incorporating the research findings into graduate courses at Wichita State University and other training events as follows:

- The principal investigator (PI) has incorporated the risk and resilience concepts into the course IME-864: Risk Analysis through projects dedicated to transportation system risk and resilience modeling and analysis.
- The PI used the battery failure simulation models as material for electrical vehicle battery failure risk analysis projects and employed the experimental data for project validation studies in the course IME-754: Reliability and Maintainability.
- The PI incorporated the electrical vehicle battery failure multiphysics simulation tool into the course IME-864: Risk Analysis. Specifically, students were able to leverage the simulation tool for the identification and forecasting of catastrophic electrical vehicle battery failures, such as thermal runaway, and the development of risk mitigation plans.
- The PI and his students have interacted with a leading company conducting battery research for medical devices, and one student (Guangxing Bai) has successfully obtained a co-op opportunity at Medtronic to conduct battery failure research.
- The PI has provided training seminars to a broader range of students and professionals through the IME colloquium, attended by graduate students from the College of Engineering at Wichita State University, local industrial professionals through the Wichita chapter of the Institute of Industrial and Systems Engineers (IISE), and local industrial advisory board members.
- Students have taken advantage of a course the PI is teaching to become involved in a project that aims to determine battery failure modes using the battery testing facilities in the PI's laboratory.
- The PI has been invited to provide two seminars, at Argonne National Laboratory and Kansas State University, respectively.

Dissemination of Results

- In this reporting period, the researchers actively disseminated the research results through the presentation of papers at relevant technical conferences, such as the IEEE Annual Conference on Prognostics and Health Management (IEEE PHM Conference).
- Meanwhile, researchers at Wichita State University have been working with a leading electronics testing company (Integra Technologies, LLC) to develop research collaborations and disseminate research results. A graduate student has obtained a co-op opportunity with another collaborator, Medtronic, to further conduct battery research on medical devices.
- The researchers also established an industrial collaboration with Medtronic to disseminate research results through seminars while also obtaining internship opportunities for graduate students.

Research Publications

Journal publications based on the results of this study are listed for Bai and Wang in the References.

Broad Impacts

With the depletion of fossil fuels and the prevalence of EVs and HEVs, attention is increasingly being paid to the application of batteries as major energy storage devices. Therefore, developing a reliable BMS that describes a battery pack's present operating conditions is a core task in current research. The BMS must be able to not only estimate values indicative of a cell's condition, which includes the battery's SoC, instantaneous available power, and SoH (such as power fade and capacity fade), but it must also capture the changing battery characteristics over time as the cell ages.

The completed research aimed to develop a novel battery health management platform that would overcome existing challenges regarding low accuracy and efficiency due to a high dependency on battery physical models that are subject to manufacturing variability and operational uncertainties. The research provides a new solution for safety-critical battery failures and will impact future transportation research by providing a better understanding of battery failure modeling and prevention. The development of this model-free battery health management system not only provides new technology for electric vehicle systems but will likely stimulate growth in several high-technology industries, such as portable mobile device manufacturing, general aviation, space exploration and travel, and more, that heavily rely on batteries as energy storage devices and that may suffer from catastrophic battery system failures at key operating stages. The research promotes the understanding of battery system failures and further opens a new research avenue to exploit innovative methodologies addressing the failure physics of battery systems and the design of new battery materials. Although the applications address critical demands in electric vehicles, the methodology is applicable to other battery applications in general.

Finally, this research offers unique findings and educational experiences for researchers across the fields of transportation systems, prognostics, and health management while providing the opportunity for training students in an interdisciplinary learning environment. A wide range of dissemination and outreach programs have been accomplished that promote data sharing, attract students to engineering careers, and broaden the participation of women and underrepresented groups.

REFERENCES

Bai, G. and P. Wang. 2014a. A Self-Cognizant Dynamic System Approach for Health Management: Lithium-Ion Battery Case Study. *Proceedings of ASME 2014 International Design Engineering Technical Conference & Computers and Information in Engineering Conference (IDETC/CIE)*, Buffalo, NY, August 17–20.

——. 2014b. Multiphysics Based Failure Identification of Lithium Battery Failure for Prognostics. *Proceedings of 2014 IEEE International Conference on Prognostics and Health Management*, Spokane, WA, June 22–25. https://ieeexplore.ieee.org/stamp/stamp.jsp?arnumber=7036389.

——. 2016a. Prognostics Using an Adaptive Self-Cognizant Dynamic System Approach. *IEEE Transactions on Reliability*, Vol. 65, No. 3, pp. 1427–1437.

——. 2016b. An Internal State Variable Mapping Approach for Li-Plating Diagnosis. *Journal of Power Sources*, Vol. 323, pp. 115–124.

Bai, G., P. Wang, C. Hu, and M. Pecht. 2014a. A generic model-free approach for lithium-ion battery health management. *Applied Energy*, Vol. 135, pp. 247–260.

Bai, G., P. Wang, and C. Hu. 2014b. A Self-Cognizant Dynamic System Approach for Battery State of Health Estimation. *Proceedings of 2014 IEEE International Conference on Prognostics and Health Management*, Spokane, WA, June 22–25.

——. 2015. A Self-Cognizant Dynamic System Approach for Prognostics and Health Management. *Journal of Power Sources*, Vol. 278, pp. 163–174.

Cai, L. and R. E. White. 2010. An Efficient Electrochemical-Thermal Model for a Lithium-Ion Cell by Using the Proper Orthogonal Decomposition Method. *Journal of the Electrochemical Society*, Vol. 157, No. 11, pp. A1188–A1195.

Charkhgard, M. and M. Farrokhi. 2010. State-of-Charge Estimation for Lithium-Ion Batteries Using Neural Network and EKF. *IEEE Transactions on Industrial Electronics*, Vol. 57, No. 12, pp. 4178–4187.

Chaturvedi, N. A., R. Klein, J. Christensen, J. Ahmed, and A. Kohic. 2010. Algorithms for Advanced Battery-Management Systems. *IEEE Control Systems*, Vol. 30, No. 3, pp. 49–68.

Doughty, D. and E. P. Roth. 2012. A General Discussion of Li Ion Battery Safety. *The Eletrochemical Society Interface*, Vol. 21, No. 2, pp. 37–44.

Forman, J. C., S. J. Moura, J. L. Stein, and H. K. Fathy. 2012. Genetic identification and fisher identifiability analysis of the Doyle–Fuller–Newman model from experimental cycling of a LiFePO$_4$ cell. *Journal of Power Sources*, Vol. 210, pp. 263–275.

Fuller, T. F., M. Doyle, and J. Newman. 1994. Simulation and Optimation of the Dual Lithium Ion Insertion Cell. *Journal of the Electrochemical Society*, Vol. 141, No. 1, pp. 1–10.

Guo, M., G. Sikha, and R. E. White. 2011. Single-Particle Model for a Lithium-Ion Cell: Thermal Behavior. *Journal of the Electrochemical Society*, Vol. 158, No. 2, pp. A122–A132.

Hu, C., B. D. Youn, and J. Chung. 2011. A multiscale framework with extended Kalman filter for lithium-ion battery SOC and capacity estimation. *Applied Energy*, Vol. 92, pp. 694–704.

Legrand, N., B. Knosp, P. Desprez, F. Lapicque, and S. Rael. 2014. Physical characterization of the charging process of a Li-ion battery and prediction of Li plating by electrochemical modeling. *Journal of Power Sources*, Vol. 245, pp. 208–216.

Miranda, Á. G and C. W. Hong. 2013. Integrated modeling for the cyclic behavior of high power Li-ion batteries under extended operating conditions. *Applied Energy*, Vol. 111, pp. 681–689.

Ning, G. and B. N. Popov. 2004. Cycle Life Modeling of Lithium-Ion Batteries. *Journal of the Electrochemical Society*, Vol. 151, No. 10, pp. A1584–A1591.

Ning, G., R. E. White, and B. N. Popov. 2006. A generalized cycle life model of rechargeable Li-ion batteries. *Electrochimica Acta*, Vol. 51, No. 10, pp. 2012–2022.

Perkins, R. D., A. V. Randall, X. Zhang, and G. L. Plett. 2012. Controls oriented reduced order modeling of lithium deposition on overcharge. *Journal of Power Sources*, Vol. 209, pp. 318–325.

Plett, G. L. 2004. Extended Kalman filtering for battery management systems of LiPB-based HEV battery packs - Part 1. Background. *Journal of Power Sources*, Vol. 134, No. 2, pp. 252–261.

Ramadass, P., B. Haran, P. M. Gomadam, R. White, and B. N. Popov. 2004. Development of First Principles Capacity Fade Model for Li-Ion Cells. *Journal of the Electrochemical Society*, Vol. 151, No. 2, pp. A196–A203.

Ramadesigan, V., V. Boovaragavan, M. Arabandi, K. Chen, H. Tsukamoto, R. Braatz, and V. Subramanian. 2009. Parameter estimation and capacity fade analysis of lithium-ion batteries using first-principles-based efficient reformulated models. *ECS Transactions*, Vol. 19, No. 16, pp. 11–19.

Santhanagopalan, S., Q. Guo, P. Ramadass, and R. E. White. 2006. Review of models for predicting the cycling performance of lithium ion batteries. *Journal of Power Sources*, Vol. 156, No. 2, pp. 620–628.

Santhanagopalan, S., Q. Guo, and R. E. White. 2007. Parameter estimation and model discrimination for a lithium-ion cell. *Journal of the Electrochemical Society*, Vol. 154, No. 3, pp. A198–A206.

Sun, Y-H, H-L. Jou, J-C. Wu, and K-D. Wu. 2010. Auxiliary health diagnosis method for lead-acid battery. *Applied Energy*, Vol. 87, No. 12, pp. 3691–3698.

Speltino, C., D. Di Domenico, G. Fiengo, and A. Stefanopoulou. 2009. On the experimental identification of an electrochemical model of a lithium-ion battery: part II. *Proceedings of the European Control Conference*, Budapest, Hungary.

Schmidt, A., M. Bitzer, A. Imre, and L. Guzzella. 2010. Experiment-driven electrochemical modeling and systematic parameterization for a lithium-ion cell, *Journal of Power Sources*, Vol. 195, No. 5, pp. 5071–5080.

Zhang, J. and J. Lee. 2011. A review on prognostics and health monitoring of Li-ion battery. *Journal of Power Sources*, Vol. 196, No. 15, pp. 6007–6014.

Zheng, Y., M. Ouyang, L. Lu, J. Li, X. Han, L. Xu, H. Ma, T. A. Dollmeyer, and V. Freyermuth. 2013. Cell state-of-charge inconsistency estimation for LiFePO4 battery pack in hybrid electric vehicles using mean-difference model. *Applied Energy*, Vol. 111, pp. 571–580.

APPENDIX A. P2D MODEL EQUATIONS

Based on principles and kinetics, equations can be presented that model the electrochemical dynamics in a Li-ion battery. By integrating Kirchoff's law with Ohm's law, the representation of the electric potential Φ_s in the solid phase can be obtained by the following:

$$\sigma_i \frac{\partial^2 \Phi_s}{\partial x^2} = a_i F j_i, \, i = p, n \tag{A.1}$$

with these boundary conditions:

$$-\sigma_i \frac{\partial \Phi_s}{\partial x}\bigg|_{x=0,L} = I, \, and \, \Phi_{s,x=0} = 0 \tag{A.2}$$

where σ represents the effective electronic conductivity of electrode i ($i = p$, n), I is the external current density, a is the specific surface area of electrode i, F is the Faraday's constant, and j is the wall flux of Li^+ on the intercalation particle of electrode i. At the interface between an electrode and current collector (i.e., x = 0), the first boundary condition in Equation (A.2) is derived because the current density in electrolyte i_e is approximated as 0. The potential in the solid phase of the negative electrode is zero as the second boundary condition. The electric potential at two ends of different electrodes can be used to calculate the following output voltage:

$$V = \Phi_{s,x=L} - \Phi_{s,x=0} \tag{A.3}$$

The potential in the electrolyte can be calculated as follows:

$$\frac{\partial \Phi_e}{\partial x} = -\frac{i_e}{\kappa} + \frac{2RT}{F}(1-t_+) \times \left(1 + \frac{d \ln f_{c/a}}{d \ln c_e}\right) \frac{\partial \ln c_e}{\partial x} \tag{A.4}$$

Since only the differences of potentials can be measured, boundary conditions can randomly be set as follows:

$$\Phi_{e,x=L} = 0$$
$$\Phi_{e,x=l_n,-} = \Phi_{e,x=l_n,+} \, and \, \Phi_{e,x=l_p,-} = \Phi_{e,x=l_p,+} \tag{A.5}$$

where κ is the ionic conductivity of the electrolyte, R is the universal gas constant, T is the temperature of the battery, F is the Faraday's constant, t_+ is Li^+ transference number in the electrolyte, and $f_{c/a}$ is the mean molar activity coefficient in the electrolyte.

According to Fick's law, the Li-ion concentration in the electrolyte is modeled as follows:

$$\frac{\partial c_e}{\partial t} = D_{eff,i} \frac{\partial^2 c_e}{\partial x^2} + a(1-t_+)j_i, \quad i = p,n \tag{A.6}$$

with initial condition:

$$c_e\big|_{t=0} = c_e^0 \tag{A.7}$$

and boundary conditions:

$$\frac{\partial c_e}{\partial x}\bigg|_{x=0,L} = 0 \text{ and } \frac{\partial c_e}{\partial x}\bigg|_{x=l_i,-} = \frac{\partial c_e}{\partial x}\bigg|_{x=l_i,+}, \quad i = p,n \tag{A.8}$$

where D_{eff} is the effective diffusion coefficient in electrolyte p, n represents the positive and negative electrodes, respectively, and a is the specific interfacial area, expressed as the following:

$$a = \varepsilon_s \left(4\pi R_p^2\right) / \left[(4/3)\pi R_p^3\right] = \varepsilon_s \left(3/R_p\right) \tag{A.9}$$

where ε_s represents the volume fraction of the solid electrode material in the porous electrode and R_p is the radius of particles in the solid phase.

In the solid phase, the transport of the Li-ion also follows Fick's law, similarly, but associates a spherical particle of R_p with each particle's location x. For each particle at location x, the Li-ion concentration is described as follows:

$$\frac{\partial c_s}{\partial t} = \frac{1}{r^2} \frac{\partial}{\partial r}\left(D_{s,i} r^2 \frac{\partial c_s}{\partial r}\right), \quad i = p,n \tag{A.10}$$

with initial condition:

$$c_s\big|_{t=0} = c_s^0 \tag{A.11}$$

and boundary conditions:

26

$$\left.\frac{\partial c_s}{\partial r}\right|_{r=0} = 0 \; and \; \left.\frac{\partial c_s}{\partial r}\right|_{r=R_p} = -\frac{1}{D_s}j_i, i = p,n$$

(A.12)

where r is the radial coordinate of particles in electrodes, R_p is the maximum radius of particles, and D_s is the diffusion coefficient in solid phase of electrodes.

Relating the net pore-wall molar flux with the divergence of the current, the relationship between them at each x location can be obtained as follows:

$$\frac{\partial i_e}{\partial x} = aFj_i, i = p,n$$

(A.13)

where ε_s is the volume fraction of the solid electrode material in the porous electrode. Besides, the solid phase intercalation overpotential η_s, which determines the rate of the intercalation reaction occuring on the surface of the solid particles, is described as follows:

$$\eta_s = \Phi_s - \Phi_e - U_r(c_{s,surf}) - FR_f j_i$$

(A.14)

where U_r represents the equilibrium potential at the existing surface concentration and R_f represents the film resistance of the SEI.

To associate all the useful variables together and compute molar flux j, the Butler-Volmer equation is employed to build the connection with them. The Butler-Volmer equation is expressed as follows:

$$j = \frac{i_0}{F}\left[\exp\left(\frac{\alpha_a F}{RT}\eta_s\right) - \exp\left(\frac{-\alpha_c F}{RT}\eta_s\right)\right]$$

(A.15)

where α_a and α_c are the transport coefficients, and i_0 is the exchange current density, which can be expressed as follows:

$$i_0 = r_{eff}c_e^{\alpha_a} \times \left(c_{s,max} - c_{s,surf}\right)^{\alpha_a} \times c_{s,surf}^{\alpha_c}$$

(A.16)

where r_{eff} is a constant and $c_{s,max}$ is the maximum concentration of Li-ion in different electrodes depending on specific material properties. Combining all the equations, the output voltage V can be solved by the given input, which is the applied current I.

THE INSTITUTE FOR TRANSPORTATION IS THE FOCAL POINT FOR TRANSPORTATION AT IOWA STATE UNIVERSITY.

InTrans centers and programs perform transportation research and provide technology transfer services for government agencies and private companies;

InTrans manages its own education program for transportation students and provides K-12 resources; and

InTrans conducts local, regional, and national transportation services and continuing education programs.

INSTITUTE FOR TRANSPORTATION

IOWA STATE UNIVERSITY

Visit **www.InTrans.iastate.edu** for color pdfs of this and other research reports.